Analysis of neutron diffraction profiles in bronze archaeological statuettes produced by solid lost wax casting

2008 J. Phys.: Condens. Matter 20 104251

(http://iopscience.iop.org/0953-8984/20/10/104251)

J. Phys.: Condens. Matter **20** (2008) 104251 (7pp) doi:10.1088/0953-8984/20/10/104251

Analysis of neutron diffraction profiles in bronze archaeological statuettes produced by solid lost wax casting

Alessandra Giuliani[1,3], Fabrizio Fiori[1], Jacqueline Gysens[2], Adrian Manescu[1] and Franco Rustichelli[1]

[1] Department of Sciences Applied to Complex Systems, Polytechnic University of Marche, Physical Sciences Section, Via Brecce Bianche, 60131 Ancona, Italy
[2] Istituto Italiano per l'Africa e l'Oriente, Roma, Italy

E-mail: a.giuliani@univpm.it

Received 16 July 2007, in final form 9 November 2007
Published 19 February 2008
Online at stacks.iop.org/JPhysCM/20/104251

Abstract
In the framework of a research aiming to assess the suitability of neutron/x-ray non-destructive techniques for the characterization of archaeological objects, two bronze items were studied by neutron diffraction. The origins of two small statues are, respectively, Egyptian (XXI–XXX Dynasties, c1070–343 B.C.) and Etruscan (IV–III centuries B.C.), belonging to a private collection. By hard x-ray diffraction we previously verified that both statuettes have a coarse microstructure (big grains). From historical considerations we believe that both items were produced by solid lost wax processes of casting. This processing technique does not completely justify the presence of microstrains; as a consequence, due to unexpected neutron diffraction peak broadening, a non-uniform Sn wt% is suspected. In the present work we discuss this deduction by means of Rietveld analysis of the neutron diffraction profiles.

1. Introduction

Devotional objects of the *ex-voto* kind, to be referred to a certain type of popular devotion within Egyptian and Etruscan religious traditions, were normally made in different materials such as stone, gold, ivory, ceramic, etc [1–3].

Small votive statuettes, such as those considered in our analysis, were apparently standardized products with a wide diffusion both during the last Pharaonic dynasties (XXI–XXX dynasties, c1070–343 B.C.) and in the Etruscan society (IV–III centuries B.C.), when they were produced for a vast clientele, belonging to the emerging 'middle class' and reflecting changed economical and political conditions [4–7]. Since the Ancient Mycenaean period, votive statuettes had normally been produced by lost wax casting in the East Mediterranean regions. This production technology reached Etruria in the last Iron Age, merging with the Villanovan traditions. In particular, the small bronze items, like those here investigated, were always prepared by full direct casting: after heating by hand, the wax was easily modelled to the desired shape (small animals, human figures, etc). Then the wax item was fully covered by several layers of clay, starting from finer clay in order to preserve the details modelled on the wax. When the clay was dried, the item was warmed up until the wax exited or evaporated: at this point the bronze alloy was strained down into the model (figure 1) [8].

For a binary copper–tin alloy, craftsmen from the 10th century B.C. had to choose the tin content of the bronze alloys on the basis of three main parameters: colour, tin cost, and forming process. Although tin was and still is an expensive metal, a high Sn content was favourable if the piece was obtained by casting, because the melting range of the alloy and the gas solubility significantly decrease with respect to pure copper [9].

In this work, we studied the composition and the microstructure in two ancient bronze votive statuettes (figure 2), using non-destructive investigation techniques such as neutron diffraction (ND). The present analysis has been performed in order to give an example of the complementarities of elemental and structural analysis, highlighting the potential insight to manufacturing details given by the latter.

[3] Author to whom any correspondence should be addressed.

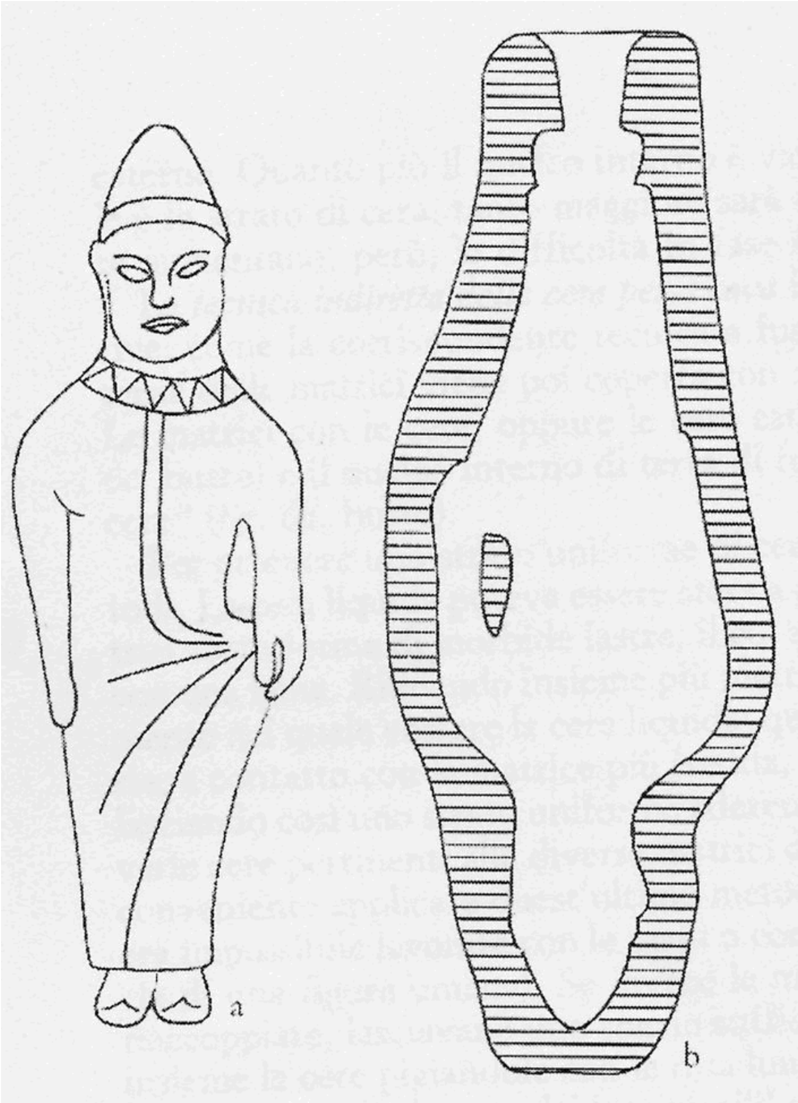

Figure 1. Direct full lost wax casting. (a) Wax model; (b) clay covering with empty internal space ready for the bronze straining. Reproduced with permission from [5].

The first object examined in the present work is a small bronze statuette (height: 55 mm; max. thickness: 5 mm) of the Ancient Egyptian civilization of unknown exact provenance and stored in a private collection. Made of solid cast bronze, it reveals a rudimentary execution but relatively good conservation. The representation refers to an episode from the mythological Delta cycle, in which Isis is known to be hiding from the God Seth's wrath in the Nile Delta's swamps, giving birth and nurturing Osiris' heir. This statuette presents stylistic features distinctive of the Late Dynastic period [1–3].

The second artefact is a small bronze statuette (height: 65 mm; maximum thickness: 5 mm) of Etruscan provenance (IV–III centuries B.C.) and stored in the same private collection. This item is also made of solid cast bronze and it is in a good state of conservation.

Due to their high penetration power, thermal and cold neutrons are a unique tool to probe metallic materials at the bulk level, and different techniques based on neutron beams are extensively used to study a wide range of materials for many applications, including cultural heritage research. In particular, in the present work neutron diffraction (ND) experiments were performed at the D1A high-resolution neutron diffractometer of the Institute Laue-Langevin (ILL) in Grenoble (F), to provide information about microstructural features arising during the manufacturing processes of the two statuettes. In fact, ND is a 'phase and structure sensitive method' that gives information on the microstructures and crystal structures of different phases in crystalline objects [10, 11]. Furthermore, neutrons are not disturbed by the surface corrosion phases, because they penetrate deep into the items, impinging relatively big volumes, thus delivering representative information on the whole bulk material.

Diffraction data were here analysed using the Rietveld refinement method [12], which allowed us to quantitatively determine the different recognized phases in different sampling volumes of the artefact bulk, putting them in correlation with the manufacturing process and the eventual thermo-mechanical treatments.

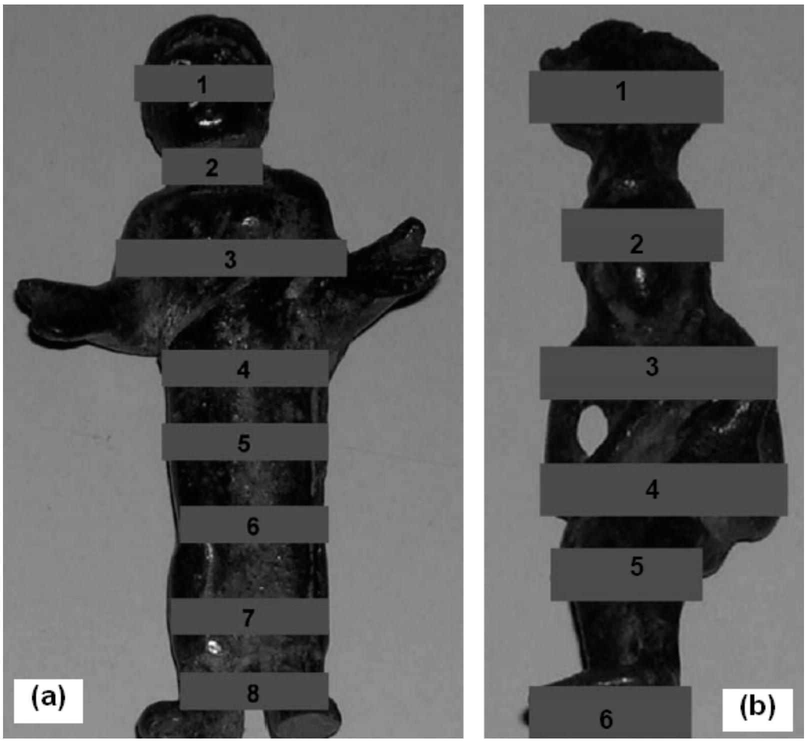

Figure 2. Etruscan (a) and Egyptian (b) statuettes. Gauge volumes in evidence.

Table 1. Composition of the two investigated items, as determined by XRF after patina removing and as the average on ten measures (values supplied in wt%—from [13]).

	Cl	Ca	Cr	Fe	Ni	Cu	Zn	As	Sn	Pb
Etruscan	0.4 ± 0.3	1.4 ± 0.9	0.08 ± 0.01	2.2 ± 0.6	0.2 ± 0.02	78.9 ± 6.1	1.1 ± 0.3	0.8 ± 0.2	6.7 ± 1.8	8.2 ± 2.2
Egyptian	—	—	0.3 ± 0.4	0.6 ± 0.6	0.2 ± 0.05	90.2 ± 1.0	0.1 ± 0.2	$<0.1 \pm 0.02$	5.3 ± 0.3	3.2 ± 0.3

2. Experiments and data acquisition

2.1. Preliminary results

A preliminary x-ray fluorescence analysis (XRF) was performed on both statuettes. XRF spectra were obtained at different positions (head, legs, bust, etc) before patina removing and under the feet of both artefacts after removing the patina in this specific area. The data in table 1 refer to the analysis performed after the removal of surface patina for both items, and the reported values are the averages of measurements in different locations of the items.

They show clearly that As was detected only on the Etruscan statue and that Pb has considerably lower concentration in the Egyptian statue. The Pb contents have to be considered overestimated in both cases because the presence of corrosion patina residues significantly raises (up to 20–30%) the measured Pb in respect to the bulk effective contents. Indeed, Cu^{2+} ions form salts, easily removable from the surface; Sn and Pb, on the other hand, oxidize, forming corrosion products that are stable and insoluble. Because of this, XRF supplies just *semi-quantitative* information on the content of the elements in the bulk.

2.2. Neutron diffraction (ND) analysis

ND experiments were carried out on the high-resolution powder and stress scanning diffractometer D1A at the Laue-Langevin Institute (ILL) in Grenoble, France (figure 3).

Eight gauge volumes centred on the 65 mm vertical axis of the Etruscan statuette (figure 2, left) and six different gauge volumes centred on the 55 mm vertical axis of the Egyptian one (figure 2, right) were analysed to determine the compositional variation of the bronze and to investigate peak broadening. For the collection of diffraction patterns, the statuettes were fixed on a sample-holder with the volume to be illuminated centred on the statue's vertical axis and covering the whole cross-section. The neutron beam size was 12×4 mm^2, obtained with suitable slits on the primary beam and the used wavelength was of 1.909 Å. Neutrons scattered by the statuettes were registered by a neutron ^{3}He multidetector. This multidetector, consisting of a bank of 25 high efficiency collimators and counters, with a large angular coverage ($20° < 2\theta < 150°$) permits rapid data collection and, above all, the refinement of up to 150 structural parameters using the Rietveld method.

For the phase analysis done with the FULLPROF software [14] the 25 multidetector elements were used to give rise to a final high-resolution diffraction pattern for each gauge volume. The observed patterns were analysed according

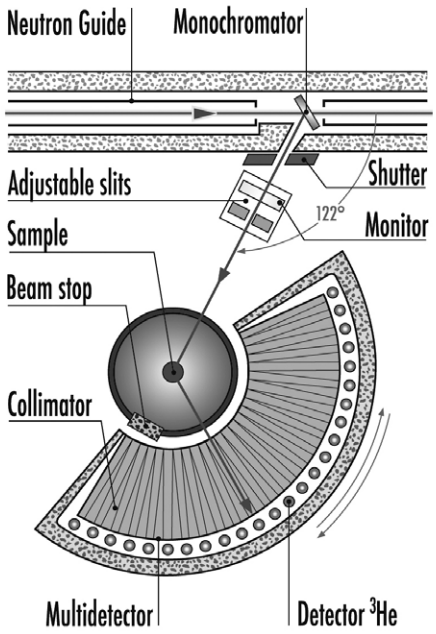

Figure 3. High-resolution powder and stress scanning diffractometer D1A beamline at the Laue-Langevin Institute (ILL).

to the Rietveld method [12] that is based on an iterative fitting process aiming to model the diffraction patterns for the crystal structures, reconstructing the identified phases. Weight fractions and the lattice parameter of the different recognized phases were refined. The peak widths were examined by a single-peak profile analysis as well as taking into account the instrumental parameters in the Rietveld analysis, already defined for the D1A diffractometer ($U = 0.1791$, $V = -0.4503$ and $W = 0.4$).

3. Data analysis and results

3.1. Neutron diffraction results and Rietveld refinement

The neutron diffraction patterns obtained at the D1A were dominated by the α-bronze peaks belonging to a copper-type face-centred cubic structure. The lattice parameter obtained from the peak positions for bronze was higher than the one for pure copper (fcc, space group $Fm3m$, lattice parameter $a = 3.6145$ Å) due to the replacement of some Cu atoms by bigger Sn atoms. The measurement of the lattice parameter shift should have permitted the estimation of the amount of the alloy element, e.g. Sn, in the bronze and in the different investigated gauge volumes indicated in figure 2.

Information extracted by means of Rietveld refinement analysis of the neutron diffraction profiles resulted in an unexpected peak broadening compared to the aluminium reference peak widths. The bronze peak was broader and more asymmetrical in comparison to the calibration peak, which exhibited the characteristic symmetric reflection profile. Peak broadening was observed for all bronze peaks of all the scans taken on both statuettes. The peak broadening may have different causes [15] such as (i) very small particle/grain sizes, (ii) microstrain broadening due to cold-working or thermal treatment, or (iii) distributions of lattice parameters of the alloy due to a strong variation of the Sn content. By hard x-ray diffraction we verified that both statuettes have a coarse microstructure (big grains), with special reference to the Egyptian item [13]. Microstrains may be induced by working processes such as cold-working, or thermal treatments such as quenching, introducing lattice defects and distributions of lattice interplanar distances around an average value, thus becoming visible as broadening of the Bragg peaks. From the historical considerations reported in section 1, we believe that both items were produced by lost wax casting [8]: this processing technique does not justify the presence of important microstrains. As a consequence, a non-uniform Sn content was suspected and verified by the Rietveld analysis.

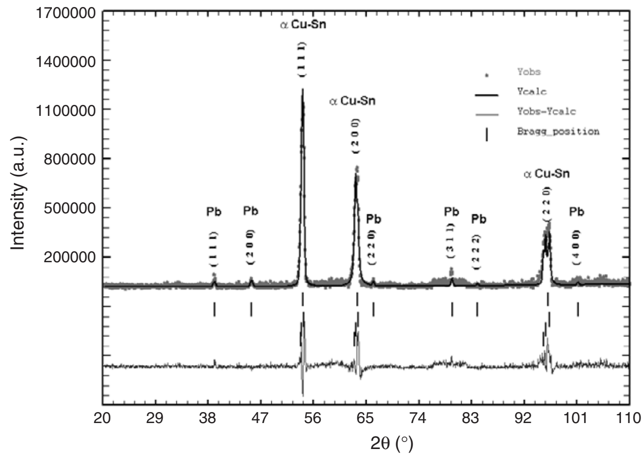

Figure 4. Diffraction pattern from the head of the Etruscan artefact.

Four different α-bronze phases were introduced in the Rietveld model, corresponding to four different lattice parameters, a. A set of four α-bronze phases plus the Pb phase were evaluated as the best choice in order to minimize the I_{obs}–I_{calc} profile for all the analysed gauge volumes and in both artefacts.

The cell parameters together with the scale factor were refined for each α-bronze phase and for the Pb phase in segregation: lead inclusions originate Bragg reflections of small intensities in the neutron patterns (fcc, $Fm3m$, $a = 4.950$ Å) of both artefacts. Figure 4 shows the profile-fitted diffraction pattern for the Etruscan statue in the head and figure 5 shows the profile-fitted diffraction pattern for the same statue but in the leg area (gauge volumes 1 and 5 in figure 2). As well, while figure 6 shows the profile-fitted diffraction pattern for the Egyptian artefact in the head-dress, figure 7 shows the same profile in the head area (gauge volumes 1 and 2 in figure 2). The other investigated gauge volumes show a similar behaviour and for this reason they are not shown or discussed. The refined lattice parameters demonstrated for both items the expansion of the copper lattice parameter that was translated into Cu and Sn weight fractions using a Vegard-type calibration curve as determined from laboratory bronze reference samples [16].

Refinement results for the Etruscan and the Egyptian items are respectively listed in tables 2 and 3. In both tables the

Table 2. Refined parameters by Rietveld analysis and derived Sn content in the Etruscan artefact.

Investigated area	a_{min} (Å)	Min. Sn content (wt%)	a_{max} (Å)	Max. Sn content (wt%)	Average Sn content (wt%)
1	3.6274	2.4	3.6557	7.8	4.5
2	3.6251	2.1	3.6559	7.8	3.3
3	3.6246	2	3.6564	7.9	3.0
4	3.6261	2.2	3.6584	8.3	3.0
5	3.6249	2	3.6578	8.2	3.5
6	3.6244	1.8	3.6563	7.9	3.5
7	3.6249	2	3.6565	8.0	4.2
8	3.6268	2.3	3.6564	7.9	3.6

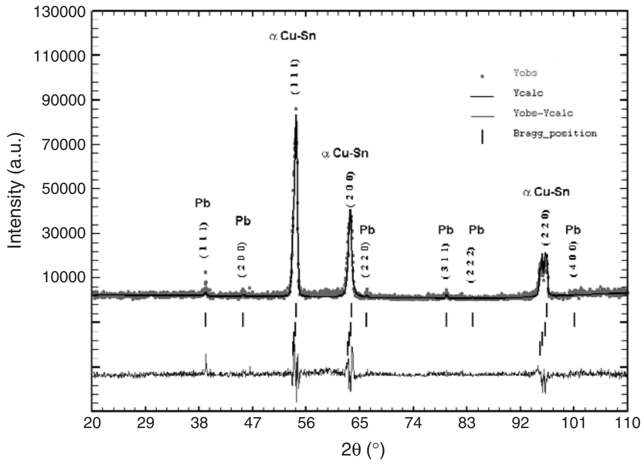

Figure 5. Diffraction pattern from the legs of the Etruscan artefact.

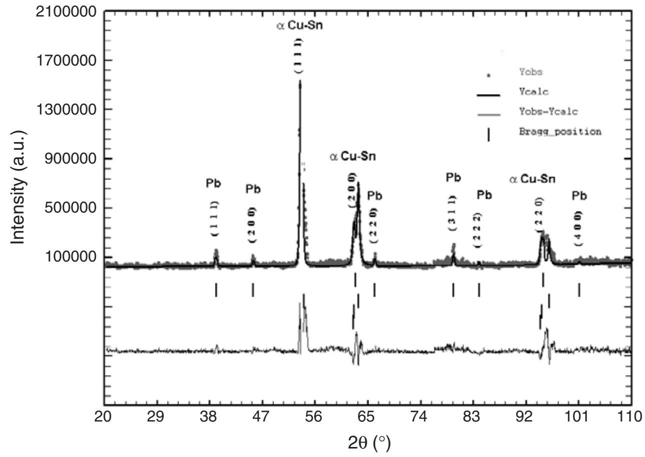

Figure 7. Diffraction pattern from the head of the Egyptian artefact.

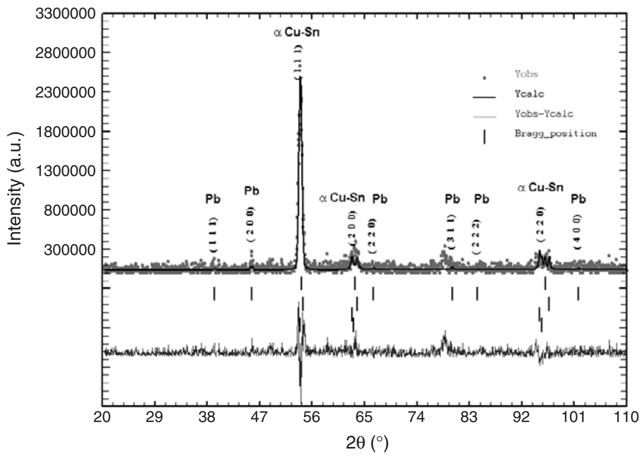

Figure 6. Diffraction pattern from the head-dress of the Egyptian artefact.

main Sn contents, listed in the last column, were obtained by a weighted averaging of the Sn wt% (extracted by means of the Vegard law) in the four α-bronze phases as a function of each phase wt%, as calculated by the Rietveld analysis.

The average Sn weight contents in the Etruscan item vary between 3 and 4.5 wt% for the analysed spots. The Egyptian item, on the other hand, exhibited distinctly different lattice parameters in the different investigated gauge volumes, indicating that the average Sn content varies between 7.7 and 14.7 wt%.

Assuming a binary Cu/Sn alloy with Pb inclusions in segregation in both artefacts, we obtained a lower Sn content in the Etruscan item than expected just on the basis of the XRF results. It is in fact assessed in the literature [17, 18] that the presence of corrosion patina highly increases the Pb and Sn concentrations and, as a consequence it reduces the Cu percentages in respect to the original alloy. In fact the Cu^{2+} ion forms salts (acetates, sulphates, carbonates) easily removable from the surface; Sn and Pb, on the other hand, oxidize forming corrosion products that are stable and insoluble. The surfacing layer thus results in lower Cu percentages and higher Pb and Sn contents.

In contrast, the Sn content in the Egyptian item is higher than expected on the basis of the XRF results: this can be explained in terms of non-uniform Sn content in the item combined with bad statistics due to the presence of fewer grains in each gauge volume. This problem seems to be connected to texture phenomena and will be faced in a future publication.

The presence of lead in segregation is confirmed in both statuettes as shown in figures 4–7. The previously reported hypothesis of a Pb content overestimation by XRF (8.2 ± 2.2 wt% in feet area) in the Etruscan statuette is confirmed by the Rietveld refinement in which lower percentages of lead were detected in the feet area (6.3 wt%—area 8 in table 4). Progressively higher Pb wt% from the head (area 1) to the feet (area 8) in the Etruscan artefact could be due to gravity effects during the solidification phase, linked to the high Pb density.

Table 3. Refined parameters by Rietveld analysis and derived Sn content in the Egyptian artefact.

Investigated area	a_{min} (Å)	Min. Sn content (wt%)	a_{max} (Å)	Max. Sn content (wt%)	Average Sn content (wt%)
1	3.6404	4.9	3.6653	9.6	7.7
2	3.6673	10.0	3.6833	13.0	10.1
3	3.6523	7.1	3.6848	13.3	8.7
4	3.6482	6.3	3.6984	15.8	14.7
5	3.6411	5.0	3.6863	13.5	12.5
6	3.6418	5.1	3.6814	12.6	11.8

Table 4. Pb content in the Etruscan artefact as derived by Rietveld analysis.

Investigated area	Average Pb content (wt%)
1	3.8
2	3.8
3	3.5
4	3.5
5	4.7
6	4.2
7	5.6
8	6.3

This hypothesis needs to be verified in other bronze artefacts produced by lost wax casting too.

The presence of Pb in the Egyptian statuette is, on the other hand, an unexpected result that can give an indication of the period in which the item was produced, i.e. during one of the last dynasties, when Pb started to be introduced in the bronze alloys in Etruria. Pb wt% in the Egyptian artefact are not reported due to the high deviation that affects the investigation reliability and that is probably linked to the coarse microstructure.

4. Conclusions

In the present work, an example of the complementarities of XRF elemental and ND structural analysis was given, highlighting the potential insight into manufacturing details given by the latter.

Although conventional XRF would have been sufficient in establishing the difference in surface elemental composition between the Egyptian and the Etruscan statuettes, the structural analysis of the bulk of the two objects required the use of neutron diffraction not normally encountered in cultural heritage studies and with which archaeologists and museum conservators are not familiar. Such non-destructive techniques relate to key issues for the future conservation of artefacts and can answer the archaeological questions about their manufacturing methods.

The neutron diffraction data analysed by the Rietveld method contain clear indications of the working processes involved in the production of the artefacts. In fact the alloy consists predominantly, in both cases, of Cu with a varying Sn content, i.e. between 1.8 and 8.3 wt% in the Etruscan item and between 4.9 and 15.8 wt% in the Egyptian one, respectively. This variation of Sn content inside the α-bronze alloy is expected if we assume, from the archaeological consideration done in section 1, that both statuettes were produced by lost wax casting. This manufacturing technique in fact foresees an uncontrolled cooling down speed of the melt; because of this, a non-uniform Sn wt% inside both statues was obtained by the Rietveld analysis.

Acknowledgments

The authors acknowledge the help of Dr T Pirling for the technical support during the neutron diffraction experiments at ILL.

This research was carried out in the framework of the Project PARNASO 'Dallo Scavo al Museo', funded by the Italian Ministry for Education, University and Research (MIUR).

This research project has been supported by the European Commission under the 6th Framework Programme through the Key Action: Strengthening the European Research Area, Research Infrastructures. Contract no: RII3-CT-2003-505925 (NMI3).

References

[1] Tran Tam Tinh V and Labreque Y 1975 *Isis Lactans. Corpus des Monuments Greco-Romains d'Isis Allaitant Harpocrate* vol 65 (Leiden: Brill Academic) pp 207–8

[2] Donadoni S (ed) 1997 *The Egyptians* (Chicago: The University of Chicago Press) pp 264–70

[3] Guidotti M C and Leospo E (ed) 1994 *La collezione Egizia del Civico Museo Archeologico di Como* (Como: Famiglia Comasca Publisher) p 74, L87

[4] Torelli M 2000 *The Etruscans. Catalogue of the Exhibition* (Palazzo Grassi: Bompiani)

[5] Cristofani M 1985 *I bronzi degli Etruschi* (Novara: Istituto Geografico De Agostini)

[6] Maetzke G 1957 *Per un Corpus dei Bronzetti Etruschi. La Collezione del Museo Archeologico Nazionale di Chiusi* vol 25 (Firenze: Istituto Nazionale di Studi Etruschi e Italici, Studi Etruschi) pp 489–523

[7] Mazzolai A 1957 *Monumenti Etruschi ed Italici nei Musei Italiani e Stranieri. Per un Corpus dei Bronzetti etruschi. La Collezione del Museo Archeologico di Grosseto* vol 26 (Firenze: Istituto Nazionale di Studi Etruschi e Italici, Studi Etruschi) pp 193–223

[8] Formigli E 1993 *Antiche Officine del Bronzo: Materiali, Strumenti, Tecniche. A cura di Edilberto Formigli* (Siena: Nuova Immagine Editrice) pp 35–53

[9] Pernot M 2000 Forming bronze by plastic deformation around the 1st millennium BC in Western Europe *J.J. Jonas Symp. on Thermomechanical Processing, Texture and Formability of Steel* ed S Yue, E Essadiqi and P Hodgson (Montreal, PQ: The Metallurgical Society of CIM) pp 615–26

[10] Kockelmann W, Kirfel A and Hähne E 2001 *J. Archaeol. Sci.* **28** 213–22
[11] Siano S, Kockelmann W, Bafile U, Celli M, Iozzo M, Miccio M, Moze O, Pini R, Salimbeni R and Zoppi M 2002 Quantitative multiphase analysis of archaeological bronzes by neutron diffraction *Appl. Phys.* A **74** (Suppl.) S1139
[12] Young R A 1993 *The Rietveld Method* (Oxford: Oxford University Press)
[13] Bastie P, Hamelin B, Fiori F, Giuliani A, Giunta G, Rustichelli F and Gysens J 2006 A new method based on hard x-ray diffraction for the investigation of archaeological artefacts *Meas. Sci. Technol.* **17** L1–3
[14] Rodrìguez-Carvajal J 2000 An introduction to the program fullprof (Available from: www.ccp14.ac.uk/tutorial/fullprof)
[15] Bunge H J 1999 *Texture and structure of polycrystals. Defect and Microstructure Analysis by Diffraction. International Union of Crystallography* (New York: Oxford University Press) p 405
[16] Siano S, Bartoli L, Zoppi M, Kockelmann W, Daymond M, Dann J A, Garagnani M G and Miccio M 2003 Microstructural bronze characterisation by time of flight neutron diffraction *Proc. Archaeometallurgy in Europe* vol 2, p 319
[17] Vittiglio G, Janssens K, Vekemans B, Adams F and Oost A 1999 A compact small-beam XRF instrument for *in situ* analysis of objects of historical and/or artistic value *Spectrochim. Acta* B **54** 1687–710
[18] Wadsak M, Constantinides I, Vitiglio G, Adriaens A, Janssens K, Schreiner M, Adams F C, Brunella Ph and Wuttmann M 2000 Multianalytical study of patina formed on archaeological metal objects from Bliesbruck–Reinheim *Mikrochim. Acta* **133** 159–64